Journal of Applied Physics

Gold and silver Schottky barriers on ZnS(110)

Cite as: Journal of Applied Physics **87**, 3905 (2000); https://doi.org/10.1063/1.372433
Submitted: 26 August 1999 . Accepted: 05 January 2000 . Published Online: 29 March 2000

D. Wolfframm, D. A. Evans, G. Neuhold, K. Horn, et al.

View Online

Export Citation

ARTICLES YOU MAY BE INTERESTED IN

The physics and chemistry of the Schottky barrier height
Applied Physics Reviews **1**, 011304 (2014); https://doi.org/10.1063/1.4858400

Effect of surface structure on workfunction and Schottky-barrier height in $SrRuO_3/SrTiO_3$ (001) heterojunctions
Journal of Applied Physics **115**, 173705 (2014); https://doi.org/10.1063/1.4872466

Electrical properties of point defects in CdS and ZnS
Applied Physics Letters **103**, 102103 (2013); https://doi.org/10.1063/1.4819492

Challenge us.
What are your needs for periodic signal detection?

Watch
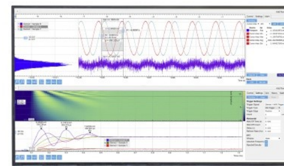
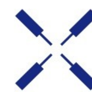
Zurich Instruments

AIP Publishing

© 2000 American Institute of Physics.

Gold and silver Schottky barriers on ZnS(110)

D. Wolfframm
Lehrstuhl Experimentalphysik II, Brandenburgische Technische Universität, Postfach 10 13 44, D-03013 Cottbus, Germany

D. A. Evans
Department of Physics, University of Wales, Aberystwyth, Ceredigion SY 23 3 BZ, United Kingdom

G. Neuhold and K. Horn[a)]
Fritz-Haber-Institut der Max-Planck-Gesellschaft, D-14195 Berlin, Germany

(Received 26 August 1999; accepted for publication 5 January 2000)

The evolution of the Schottky barrier between Au and Ag metal films and ZnS(110) has been studied using photoemission. Clean and well-ordered ZnS(110) surfaces were prepared by molecular beam epitaxy on cleaved GaP(110) surfaces. Chemical reaction and/or intermixing between the metal and substrate were not observed upon room temperature deposition. Substrate Zn $3d$ attenuation plots indicate that an initial layer-by-layer growth is followed by island growth at higher depositions. The Schottky barrier heights were found to be $\phi_B^{\mathrm{Au}}=2.19$ and $\phi_B^{\mathrm{Ag}}=1.81\,\mathrm{eV}$, indicating a considerable dependence on metal work function. This observation agrees well with predictions of Schottky barrier heights based on the concept of metal-induced gap states and the influence of charge transfer based on electronegativities, and discussed in the light of current concepts of Schottky barrier characteristics. © *2000 American Institute of Physics.*
[S0021-8979(00)00908-7]

I. INTRODUCTION

A study of the properties of metal contacts to wide band gap semiconductors serves a dual purpose. On the one hand, data are provided to investigate whether the concept of metal-induced gap states (MIGS)[1–3] which provides a satisfactory description for barrier height data of metals on III–V semiconductors, can be extended to semiconductors which have a fundamental band gap so large that the density of MIGS is too low to play an important role in pinning the Fermi level. On the other hand, contacts to wide band gap semiconductors such as II–VI compounds or the group III-nitrides are of central importance to the application of these materials in optoelectronic and other devices. In spite of this interest, only a few studies of metal deposition on wide band gap semiconductors under clean and atomically well-ordered conditions exist, and the evolution of the Fermi level from the first atomic layer onwards has been investigated in few of these, in stark contrast to the hundreds of studies on III–V materials.[4]

Here we report on a photoemission study of Au and Ag films on ZnS(110) which, with its wide fundamental band gap of 3.68 eV can be regarded as a model for the class of wide band gap III–V semiconductors. In order to avoid the problem of charging when applying electron spectroscopies to this material for which conducting samples are not readily available, we have deposited epitaxial films of ZnS on cleaved GaP(110) surfaces, where charging can be avoided by tunnelling through the film. This cubic system exhibits a lattice mismatch of only about 0.7%, and we have shown in two previous studies that well-ordered and stoichiometric films of ZnS can be prepared in this way.[5,6] Another aspect of metal-semiconductor formation also merits attention: Ohmic contact formation. In III–V compound semiconductors ohmic contact formation is based on transition metal alloy diffusion into the *p*-type film surface.[7,8] This forms a thin, highly doped region near the interface which overcomes the fundamental property that all metals on materials such as GaAs lead to a rather high Schottky barrier height.[9] A knowledge of intermixing effects and the formation of alloys between the metal and the II–VI is thus crucial in understanding factors important in contact formation. In studies of noble metals on ZnSe,[10] the most commonly used metal (Au) has been shown to form abrupt interfaces even after annealing. Interfaces formed by the deposition of several metals on ZnS were studied by Brillson[11] and showed that most of the interfaces are not abrupt. In addition, several investigations have shown that the Schottky barrier height for different metals on wide-band gap ionic semiconductors such as ZnSe[10] and ZnS[12] appears to be *more* dependent on the metal work function than for more covalent semiconductors such as GaAs or GaP. In order to investigate effects such as interface abruptness, the formation of alloys, the interdiffusion of metal and II–VI species, the stability of the metal layer, deposition studies of gold and silver onto ZnS, and annealing experiments were carried out.

In all experiments, severe surface photovoltage effects[13] were found even at room temperature. However, the equilibrium Fermi level position could still be extracted from data where the overlayer exhibits metallic character, i.e., a clear Fermi edge, and meaningful bond bending data are accessible even in the presence of a strong surface photovoltage.[14,15]

[a)]Electronic mail: horn@fhi-berlin.mpg.de

 © 2000 American Institute of Physics

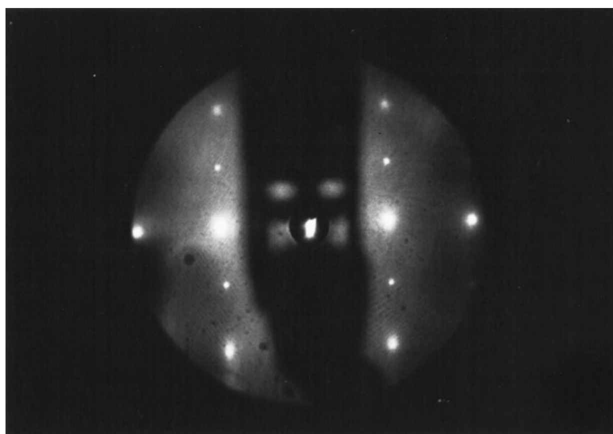

FIG. 1. LEED pattern of a clean ZnS(110) film of 85 Å thickness, deposited onto cleaved GaP(110), recorded at an electron energy of 75 eV.

II. EXPERIMENTAL PROCEDURE

The photoemission experiments were carried out on station TGM4 at BESSY (Berliner Elektronen-Speicherring-Gesellschaft für Synchrotronstrahlung mbH). The Zn $3d$, Au $5d$, and Ag $4d$ levels were accessible using the available photon energy range and the photoemission spectra for these levels were taken at normal emission using a photon energy of 43 V. The spectral resolution was approximately 110 meV; from statistical considerations it is important to stress the fact that peak and band edge positions are determined with a spectral resolution which we estimate to be $(110/\sqrt{n})$ meV, where n is the number of points utilized to measure spectral features; n is on the order of 5–30 in the present case. In addition, relative changes in Fermi level and band edge positions could be monitored by recording valence level emission spectra for the samples and a reference metal surface.

All experiments were performed in an UHV chamber equipped with low-energy electron diffraction (LEED) optics, a tool to cleave the GaP(110) crystals (MCP Ltd., UK; $N_D = 4\times10^{17}\,\mathrm{cm}^{-3}$), a temperature-controlled manipulator, ZnS and metal evaporation cells, and a high-resolution angle-resolving electron energy analyzer (HA 50, VSW Ltd., UK). After cleaving the GaP(110) crystals using a double wedge technique, a thin ZnS layer (ZnS-purity 99.999%; crystal GmbH, Berlin, Germany) was grown at a substrate temperature of 150 °C as measured by a chromel-alumel thermocouple fixed onto the sample holder. The ZnS material was evaporated from a water-cooled compound Knudsen cell at 685 °C cell temperature, giving a growth rate of ~2 Å per minute measured by a quartz crystal thickness monitor. This growth procedure gave rise to distinct features in the valence band photoelectron spectrum, and sharp LEED spots as shown by the diffraction pattern depicted in Fig. 1. Gold and silver were evaporated from water-cooled Knudsen cells, and were deposited at rates between 0.9 and 1.6 Å per minute, onto samples held at room temperature.

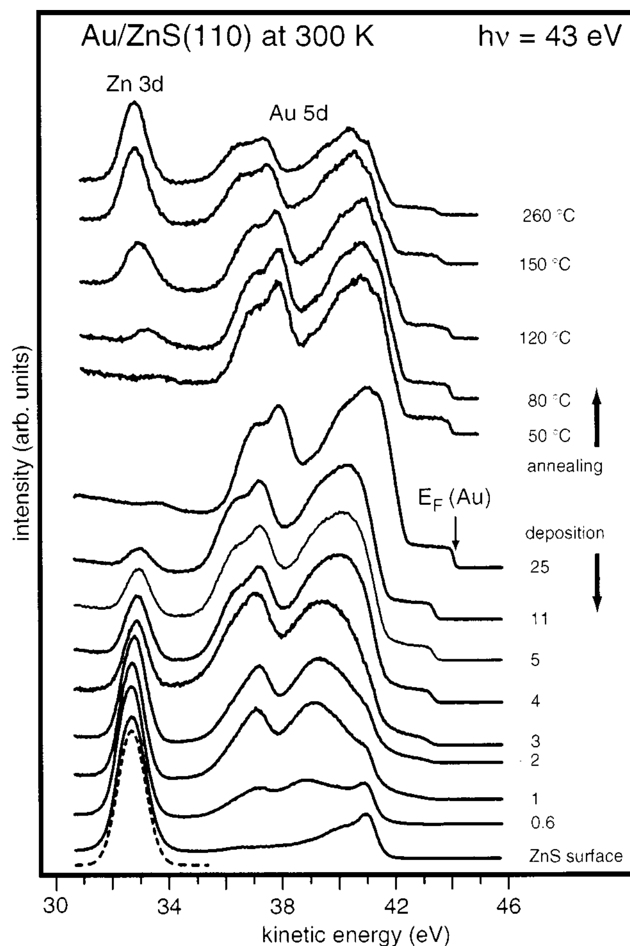

FIG. 2. (bottom): Photoelectron spectra recorded at a photon energy of 43 eV for the ZnS(110) surface as a function of gold coverage as shown on the right hand side in angstroms. The appearance of a Fermi level at 2 Å indicates the evolving metallic nature of the overlayer. The Zn $3d$ bulk component is shown for the clean ZnS(110) surface (bottom spectrum, short dashed line). The SPV breakdown appears between 11 and 17 Å. (top): Spectra from Au/ZnS(110) as a function of annealing temperature. Up to 120 °C annealing temperature the Zn $3d$ level intensity increases gradually as regions of the substrate are uncovered. Above this temperature the increase becomes much stronger and reaches a more constant value above 150 °C.

III. RESULTS AND DISCUSSION

A. Au on ZnS(110)

The characterization of overlayer growth mode and interface reactions through photoemission is generally based on an examination of core-level line intensities and peak shapes. In the present system, and under our experimental conditions, this is hampered by the fact that the sulphur core level was outside the range of photon energies provided by the monochromator. We thus had to rely on the Zn $3d$ level, which has some valence character, and exhibits evidence for subtle dispersion effects.[6] However, these are small enough that the Zn $3d$ intensities can still be used for a determination of the growth mode.

Figure 2 shows a set of spectra covering an energy range which includes substrate Zn $3d$ and overlayer Au $5d$ levels as well as the remaining valence band region. The bottom spectrum corresponds to an 80-Å-thick ZnS layer deposited

onto cleaved GaP(110) surface (clean ZnS). A wide energy range spectrum did not show any Ga $3d$ emission intensity at this coverage, indicating that the GaP(110) substrate was completely buried by ZnS. The Ga $3d$ core level attenuation confirms layerwise growth.[5] The LEED pattern showed the expected (1×1) reconstruction with sharp spots and low background which confirmed the high quality of the grown ZnS layer (Fig. 1). The Zn $3d$ emission peak in Fig. 2 could be fitted using a single peak (short dashed line), which does not gain any extra components during exposure of the surface to Au at 300 K. This suggests that the Au film does not severely disrupt the ZnS surface, although it is fair to say that this information cannot be incorporated into the analysis of the line shape since it contains band-like features,[5] such that this line cannot be modeled by an analytical line shape as in the case of a deeper core level. In the absence of further accessible core levels, this could not be confirmed from the photoelectron spectra (PES), although similar behavior is reported for Au on ZnSe, where the absence of interface reaction has been confirmed by high-resolution transmission electron microscopy.[10]

The decrease of the Zn $3d$ level intensity and the increase of the Au $5d$ level intensity with increasing Au thickness can clearly be seen in Fig. 2. The attenuation of the Zn $3d$ level intensity and the increase of the Au $5d$ intensity as a function of increasing metal coverage are shown in Fig. 3(a). The shape of the Zn $3d$ level attenuation curve changes considerably at 3 Å Au coverage. This indicates that after approximately 2 ML, the growth mode changes from a layerwise to an island-type growth, thus a coverage of 25 Å a small Zn $3d$ peak is still visible (Fig. 2). The increasingly metallic nature of the film is reflected in the appearance of a Fermi level emission $[E_F(\mathrm{Au})]$ between 2 and 3 Å. This broad edge sharpens as the coverage is increased, and is fully developed at 4 Å, suggesting that the layer has metallic character at this point. There is a slight shift of all spectra during the initial stage of growth until 3 Å coverage, which is caused by band bending. Beyond this coverage, the position of the Zn $3d$ level does not change until at a coverage of 17 Å the entire spectrum shifts to lower binding energy. This shift is caused by the reduction of the surface photovoltage (SPV), induced by the photon beam, a phenomenon that is well known in photoemission studies from metal-semiconductor interfaces, particularly in wide band gap semiconductors.[13–15] The reduction in SPV observed between about 11 and 25 eV is caused by the surface being short circuited through a contiguous metallic film,[16,17] which manifests itself as an apparent step-like change in the Fermi level position.[13] Due to the high film resistivity and Au clustering, this photovoltage breakdown occurs at 17 Å, which is significantly higher than the coverage for which the Au film appears metallic. It is interesting that this short circuiting is not brought about by the first monolayer which, from the attenuation plot in Fig. 3(a) grows in a layerwise mode. That this first layer actually has a different structure than bulk Au is in fact also evident from the shape of the Au $5d$ core level, which only develops its characteristic structure beyond 4 Å deposition (Fig. 2).

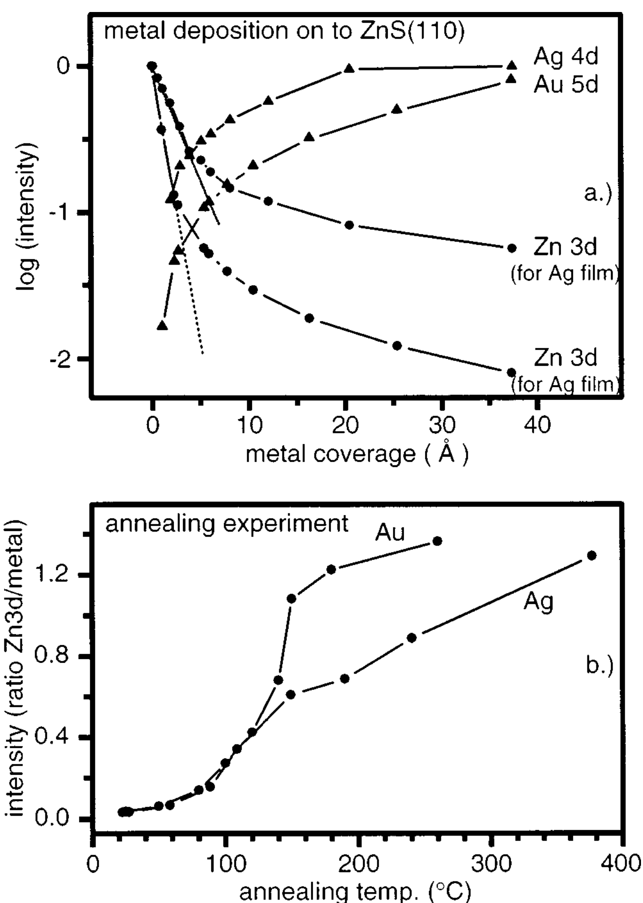

FIG. 3. (a) Relative changes in the intensities of the Zn $3d$ level, Au $5d$, and Ag $4d$ levels as a function of metal deposition, indicating layerwise growth up to a bout 3 Å and island growth at higher depositions. (b) Zn $3d$/metal d intensity ratio as a function of annealing temperature.

In order to investigate the stability of the grown Au layer, the sample was annealed at different temperatures. The corresponding spectra are shown in the top part of Fig. 2. For each step, the sample was kept for 5 min at the temperature indicated. At 50 °C, an increase in the Zn $3d$ emission intensity is already noticeable. At higher annealing temperatures (up to 120 °C), the Zn $3d$ level intensity increases gradually, suggesting that regions of the substrate are uncovered. Above this temperature, the Zn $3d$ intensity increases dramatically as shown in the plot of Fig. 3(b). Above 180 °C the Zn $3d$ to Au $5d$ intensity ratio does not vary as rapidly. This can be interpreted in several ways. The reappearance of the substrate emission peaks can be due to overlayer desorption, clustering, or indiffusion. Since the latter is likely to involve changes in the substrate core level binding energies, this is believed unlikely. Desorption is also unlikely at these relatively low temperatures, and thus we infer that the increased Zn $3d$ signals is a result of Au clustering.

The reduced conductivity of the metal film at higher temperatures is reflected in the shift to higher binding energy of the whole spectrum, indicating a re-establishment of the SPV. This also coincides with the maximum increase in Zn intensity. The difference of the $E_F(\mathrm{Au})$ position between 120 and 150 °C amounts to 0.4 eV. The value is equal to that obtained for the SPV in the set of spectra taken in the Au

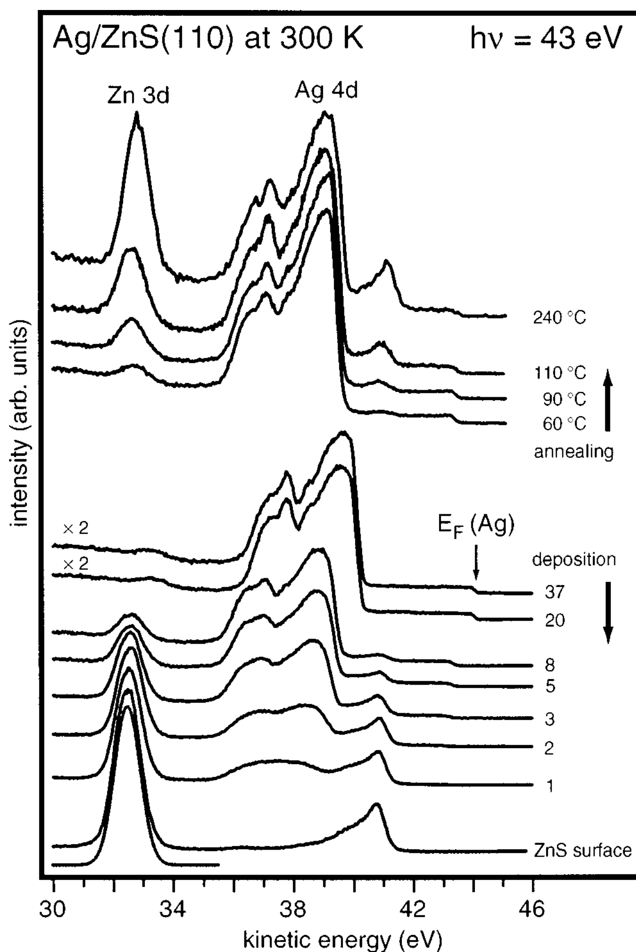

FIG. 4. (bottom): Spectra taken at a photon energy of 43 eV for the ZnS(110) surface as a function of silver coverage as shown in angstroms. The surface Fermi level appears after 2 Å coverage indicating the metallic character of the growing layer. The bottom spectrum shows the Zn 3*d* bulk component of the clean ZnS(110) surface (short dashed line). The SPV breakdown appears between 12 and 20 Å. (top): PES taken at a photon energy of 43 eV for the Ag/ZnS(110) interface as a function of annealing temperature. The absolute intensity ratio Zn 3*d* to Ag 4*d* is represented as plot in the inset as a function of annealing temperature.

deposition thickness sequence. At higher temperatures, the stable Au–ZnS surface exhibits a sharp (1×1) LEED pattern with low background similar to the one for the clean surface shown in Fig. 1. This indicates that the annealing process does not disrupt the ZnS surface.

B. Ag on ZnS(110)

The results for Ag deposition onto clean ZnS(110) give a generally similar picture compared to Au/ZnS(110). A set of spectra including the Zn 3*d* level, the Ag 4*d* level, and the ZnS valence band region is shown as a function of silver layer thickness in Fig. 4. The Zn 3*d* level of the clean ZnS surface (bottom spectrum; ZnS layer thickness = 87 Å) and the Zn 3*d* levels after Ag deposition were fitted using a single Gaussian peak (short dashed line). After the first Ag deposition of 0.5 Å the spectrum shifted about 0.2 eV to higher binding energy due to band bending. At a coverage of 2 Å the line shape of the Ag 4*d* can be seen. The surface Fermi level E_F(Ag) of the growing silver layer appears between 2 and 3 Å. This behavior is similar to that obtained for silver on ZnSe.[8] The following coverages lead to a decrease of the Zn 3*d* intensity and an increase of the Ag 4*d* intensity as expected. The line shape of both the Zn 3*d* and the Ag 4*d* level did not change. The SPV breakdown was obtained following a total coverage of 20 Å which is similar to Ag grown on ZnSe(001). The amount of the SPV evaluated for silver was higher than that for the gold. Even after a coverage of 37 Å, the Zn 3*d* level is not buried which suggests a higher degree of islanding for silver.

The intensity of the Zn 3*d* and Ag 4*d* as a function of Ag layer thickness is shown in a semilogarithmic plot in Fig. 3(a) and clearly shows a change of the growth mode at about 3 Å (~2 ML) from a layerwise to an island growth mode. Compared with Au/ZnS(110) it appears that the attenuation of the Zn 3*d* signal as a function of Ag deposition is much slower, while at the same time the Ag signal saturates much faster. This can be explained by a formation of Ag clusters which are much larger in diameter than those from Au, since due to the small electron mean free path at the photon energy employed, the Ag signal will saturate faster while larger areas of the substrate are free of metal. The clustering observed at elevated temperatures as discussed later, also occurs at room temperature, as evident from our experiment in which a Ag layer of 20 Å deposition was left at room temperature for 240 min. This lead to a doubling of intensity of the Zn 3*d* line, and the reappearance of valence band features, combined with an increase of SPV.

The rearrangement in the Ag layer upon annealing can be identified on the basis of the spectra in the upper part of Fig. 4. Annealing up to 60 °C leads to a shift of the entire spectrum to higher binding energy. This indicates that the SPV reappearance has already happened at this relatively low annealing temperature, in agreement with the change of the line shape at RT, indicating a more loosely bonded silver layer on the ZnS substrate which is similar to results obtained for Ag growth on ZnSe(001).[8] Further annealing up to 240 °C did not show any significant changes in the line shape, except the clear formation of the ZnS valence band feature.

The intensity ratio Zn 3*d* to Ag 4*d* as a function of annealing temperature is represented in Fig. 3(b). The line shape looks similar to that obtained for gold until 190 °C, but above this temperature the Zn 3*d* intensity increases significantly.

C. Fermi level shift and determination of Schottky barrier height

The data for metal deposition onto ZnS(110) in Figs. 2 and 4 can be used to determine the position of the Fermi level in ZnS(110), which is plotted in Fig. 5 as a function of metal deposition. Open symbols represent data uncorrected for SPV, while full symbols show corrected data; these latter were derived from film thicknesses where a clear Fermi edge was present in the spectra. There is a difference in initial Fermi level pinning on the clean ZnS(110) surface for the two sets of data shown here. Little is known about surface states on the clean ZnS(110) surface, but in line with the other zinc-blende-type compound semiconductors, one

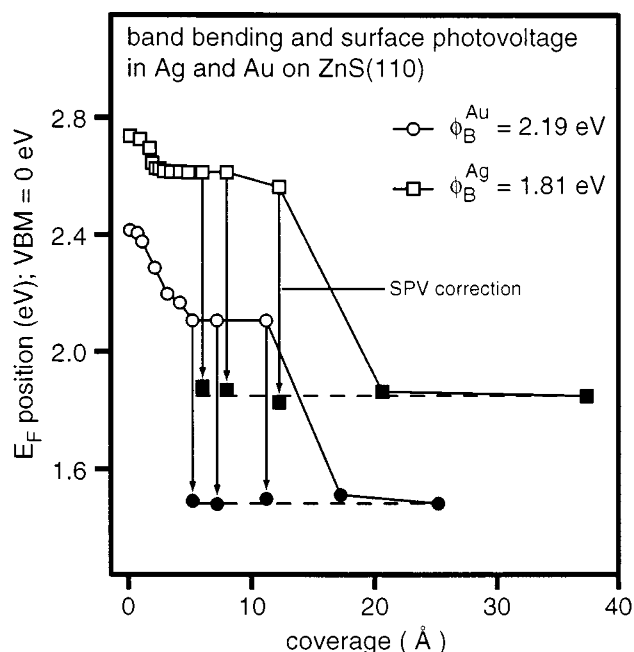

FIG. 5. Movement of the apparent surface Fermi level (open symbols) and after correction for surface photovoltage (filled symbols). Also indicated are the final barrier heights.

would expect that the bond-angle rotation relaxation sweeps surface states out of the fundamental band gap. Thus, it is likely that the observed differences in initial pinning are caused by slight differences in stoichiometry, surface order in these molecular beam epitaxy (MBE)-grown samples, or even the density of steps in the underlying GaP substrate. It would, however, be interesting to investigate whether an unoccupied surface state is responsible for Fermi level pinning, as in the case of GaP(110).[18] The different initial pinning had no influence on the measured ZnS/GaP valence band offset, nor on the final Fermi level position and Schottky barrier height. For both metals silver and gold band bending is seen up to a coverage of about 3 and 5 Å, respectively. Above this coverage the Fermi level remains constant up to approximately 10 Å. Between 10 and 20 Å the Fermi level shows an apparent shift, indicating the breakdown of the SPV. Finally, the Fermi level reaches a stable position which is equal to the reference Fermi level. The general change of the surface Fermi level position for both metals is similar to that obtained for the growth of Au on ZnSe(001) and Ag on ZnSe(001).[10] In spite of these similarities there are slight differences, e.g., in the extent of band bending as a function of metal coverage in particular. For Ag as well as Au grown on ZnS(110) the SPV breakdown is completely finished at about 20 Å metal coverage, whereas a higher coverage is necessary for both metals grown on ZnSe(001).

In order to determine the amount of surface photovoltage, the positions of the Zn $3d$ level, the valence band maximum for the clean ZnS surface and the reference Fermi level were used. Thus, the energy between Zn $3d$ and Fermi level was known. Using the shift of the Zn $3d$, the corrected points (solid symbols) could be calculated.

The Schottky barrier heights ϕ_B evaluated from these data are indicated in Fig. 5 for each metal. We find $\phi_B(\mathrm{Au})=2.19\pm0.10$ and $\phi_B(\mathrm{Ag})=1.81\pm0.10\,\mathrm{eV}$. These values are slightly higher than those from the literature[19] [$\phi_B(\mathrm{Au})=2.00$, and $\phi_B(\mathrm{Ag})=1.65\,\mathrm{eV}$], based on transport measurements. The differences of about 0.18 eV are most likely caused by the use of different methods (i.e., $I-V, C-V$) to determine ϕ_B, and different surface preparation techniques (e.g., surface etching, cleaving) prior to metal growth. Similar differences (~0.30 eV) between published data and ϕ_B values were found for gold as well as silver grown on ZnSe(001).[8] An influence of lateral barrier height inhomogeneity can also not be ruled out.[20]

The influence of those properties of the semiconductor and metal which determine the Schottky barrier heights are well understood by now (see Ref. 21 and references therein). The metal wave functions in the energy range of the semiconductor band gap tail into the latter, creating what has been named (MIGS).[2] These states are derived from the continuum of evanescent gap states, and their character changes from donor-like near the top of the valence band, to acceptor-like near the bottom of the conduction band. The energy level at which their dominant character changes is called the branch point, and it represents the reference level for the alignment of the Fermi level. The net charge in these interface states is positive (negative) if the branch point is above (below) the Fermi level. The interface state concept thus also accommodates the effect of charge transfer in the chemical bond between metal and semiconductor at the interface, which may be described in an overall manner by the electronegativity difference of the elements involved on either side of the interface. Thus, a (hypothetical) nonpolar bonding situation at the interface would give rise to a Schottky barrier height which arises from an alignment of the Fermi level with the branch point of the metal-induced gap states, i.e., its energy distance from the conduction band minimum for *n*-type material. The influence of charge transfer causes the Schottky barrier heights to be smaller (larger) if the electronegativity difference between metal and semiconductor is negative (positive). These general ideas have been put on a quantitative basis by a consideration of data for a wide range of barrier heights measured on contacts prepared under well-defined conditions as reported in the literature, by Mönch.[20] He also showed that details of the interface, such as the formation of dipole layers through specific surface structures, e.g., the stacking fault in the Si(111)-(7×7) surface, can be understood. This ''MIGS plus electronegativity'' interpretation, which has been supported by an analysis of a large body of experimental data,[3] obviously rules out a concept of two different classes of metal-semiconductor interfaces, i.e., ''covalent'' versus ''ionic,'' with a sharp transitions between the two, such as put forward by Kurtin *et al.*[21]

Returning to analysis of Schottky barrier heights for metals on ZnS, we note that our present data are a useful test for the predictions of the MIGS plus electronegativity model since they represent a case in which charge transfer is expected to be more important than in semiconductors with a smaller gap. The density of interface states (MIGS), and thus their ability to dominate the alignment of the branch point with the Fermi level, against the influence of charge transfer

TABLE I. Work function, Schottky barrier heights, and metal electronegativities for Ag and Au on ZnS. The Schottky barrier heights were derived form photoemission on ZnS(110) (this work), and by transport measurements (see Ref. 19).

Metal	Work function	Φ_B (metal/ZnS) (eV) (this work)	Φ_B (metal/ZnS) (eV) (from Ref. 19)	X (Pauling's)
Au	5.10	2.19	2.00	2.4
Ag	4.41	1.81	1.65	1.9

between metal and semiconductor, is much lower than in semiconductors with a smaller gap. Since the work functions of metals as well as the dielectric work functions of semiconductors vary linearly as a function of the corresponding electronegativities, it is not surprising that there is a work function dependence of the barrier height. While for a high density of MIGS, their influence will dominate, a low density accentuates the influence of the electronegativity difference and thus the work function difference. This relation can be written as

$$\Phi_{\mathrm{Bn}}=\Phi_{\mathrm{bp}}+S_x(X_m-X_s), \tag{1}$$

where Φ_{Bn} is the Schottky barrier height for a n-type semiconductor, Φ_{bp} is the energy of the MIGS branch point, and X_m and X_s are the metal and semiconductor electronegativities, respectively. S_x is the so-called slope parameter, which describes the dependence of the barrier height on metal electronegativity (and thus work function). It is related to the density of MIGS, the thickness of the dipole layer at the interface, and an appropriate interface dielectric constant.[3,20] The slope parameter thus describes the relative importance of the charge transfer and the MIGS.

Comparisons of this type for ZnS have so far been based on $I-V$ or $C-V$ measurements in which the stoichiometry, order and cleanliness of the semiconductor surface prior to metal deposition was not well defined.[22] Hence, it is interesting to derive the value of the S parameter from our present data, even though we only cover a limited range of metal work function. For the values in Table I, we derive a value for the S_x parameter $S_x=d\Phi_{\mathrm{Bn}}/dX_m$ of 0.76, using Pauling's electronegativities ($X_m^{\mathrm{Ag}}=1.9$ and $X_m^{\mathrm{Au}}=2.4$). We cover a considerable range of work functions (0.7 eV), on the basis of two metals where no strong interface reaction occurs which might influence the magnitude of the barrier height.

For a comparison of our experimental values with the predictions,[20,23,24] we take the branch point energy of the continuum of interface-induced gap states from Mönch[23] obtained from empirical tight binding calculations; these yield $\Phi_{\mathrm{bp}}=2.05$ eV above the valence band maximum. The slope parameter S_x is related to the density of states of the MIGS and the effective width of the dipole layer. Mönch has derived a relation between the slope parameter and the semiconductor dielectric constant ϵ_∞, on the basis of screening lengths approximated from Thomas–Fermi screening, and the decay lengths in the semiconductor which are related to the width of the band gap.[24] This relation predicts, for ZnS with a value of $\epsilon_\infty=5.2$,[25] a slope parameter of 0.64 for Pauling's electronegativities, i.e., quite close to our experimental value, and clearly in the range where the work function or electronegativity differences of the metal have a sizeable influence on the Schottky barrier height. Barrier heights may then be calculated from Eq. (1) on the basis of the predicted S parameter, which yields $\phi_B(\mathrm{Au})=2.22$ and $\phi_B(\mathrm{Ag})=1.93$ eV, i.e., again quite close to the experimental values. This good agreement lends support to the predictive character of the model based on the density of interface states and the influence of charge transfer across the interface on the magnitude of the Schottky barrier.

It is fortunate that self-consistent pseudopotential calculations of metal interaction with the ZnS(110) surface have been carried out by Louie *et al.*[26] Their results offer an intuitive explanation for the differences in Fermi level pinning observed in semiconductors with different electronic structure and magnitudes of the fundamental band gap. These authors studied the interface between aluminum (modelled by jellium) and the (110) surfaces of GaAs ZnSe, and ZnS. In their calculations of the interface density of states in the band gap region, they find that the density of these metal-induced gap states is quite low for ZnS, being much higher for Si, GaAs and ZnSe. Moreover, the penetration of these states into the semiconductor falls from 3.0 Å for Si and 1.9 Å for ZnSe to only 0.9 Å for ZnS. The authors used these results to calculate the Schottky barrier heights. They also used a simple model to relate the MIGS surface density of states and the penetration depth to the dipole potential at the surface. For ZnS they find an S parameter of $S\sim0.7$, quite close to our data from photoemission measurements above. While the calculations of Louie *et al.* are for ''jellium''-metal, they lend themselves to a comparison with our data of the noble metals, with their purely *s-p* density of states at E_F. We thus conclude that our photoemission data from metal deposition onto clean, well-defined ZnS(110) surfaces performed under UHV conditions strongly support the notion that the low density of metal-induced gap states in ZnS lead to a strong dependence of Schottky barrier heights on metal work function, in agreement with the general concepts based on electronegativity considerations,[3,20,23,24] and the theoretical description of the metal-ZnS bond.[26]

ACKNOWLEDGMENTS

The authors gratefully acknowledge the technical support by H. Haak and the staff of the Berliner Elektronen-Speicherring-Gesellschaft für Synchrotronstrahlung (BESSY) for their assistance. D. W. would also like to thank C. J. Dunscombe, University of Wales College of Cardiff, for his helpful discussions given during the analysis of the experiments. This work was supported through Bundesministerium für Bildung und Forschung under Grant No. 05-622 OLA 3, and through European Community HCM-LSI program, Contract No CHGE-CT93-007.

[1] V. Heine, Phys. Rev. A **138**, 1589 (1961).
[2] J. Tersoff, Phys. Rev. Lett. **52**, 652 (1984).
[3] W. Mönch, Rep. Prog. Phys. **53**, 221 (1990); W. Mönch, *Advances in Solid State Physics* (Festkörperprobleme, to be published).
[4] E. H. Rhoderick and R. H. Williams, *Metal-semiconductor interfaces* (Oxford Science Publications, Oxford, 1988).

[5] D. Wolfframm, P. Bayley, D. A. Evans, G. Neuhold, and K. Horn, J. Vac. Sci. Technol. A **14**, 844 (1996).
[6] S. R. Barman, S.-A. Ding, G. Neuhold, K. Horn, D. Wolfframm, and D. A. Evans Phys. Rev. B **58**, 7053 (1998).
[7] A. G. Milnes and D. L. Feucht, *Heterojunctions and Metal-Semiconductor Junctions* (Academic, New York, 1972).
[8] F. Schäffler and G. Abstreiter, J. Vac. Sci. Technol. B **3**, 1184 (1985).
[9] A. B. McLean and R. H. Williams, J. Phys. C **21**, 783 (1988).
[10] D. A. Evans *et al.*, Appl. Surf. Sci. **104/105**, 240 (1996).
[11] L. J. Brillson, Thin Solid Films **89**, 461 (1982).
[12] J. M. Dharmadasa, W. G. Herrenden-Harker, and R. H. Williams, Appl. Phys. Lett. **48**, 1082 (1986).
[13] M. Alonso, R. Cimino, and K. Horn, Phys. Rev. Lett. **64**, 1947 (1990).
[14] K. Horn, Surf. Sci. **269/270**, 938 (1992); K. Horn, M. Alonso, and R. Cimino, Appl. Surf. Sci. **56–58**, 271 (1992).
[15] P. Chiaradia, J. E. Bonnet, M. Fanfoni, C. Goutti, and G. Lampel, Phys. Rev. B **47**, 13520 (1993).
[16] M. H. Hecht, Phys. Rev. B **41**, 7918 (1990).
[17] D. A. Evans, T. P. Chen, T. Chassé, and K. Horn, Appl. Surf. Sci. **56–58**, 233 (1992).
[18] D. Straub, M. Skibowski, and F. J. Himpsel, J. Vac. Sci. Technol. A **3**, 1484 (1985).
[19] Landolt-Börnstein, *Numerical Data and Functional Relationships in Science and Technology, II–VI Compounds*, edited by M. Helbig (Springer, Berlin, 1982), Vol. 17d, Chap. 6.4, p. 190.
[20] W. Mönch, J. Vac. Sci. Technol. B **17**, 1867 (1999).
[21] S. Kurtin, T. C. McGill, and C. A. Read, Phys. Rev. Lett. **22**, 1433 (1969).
[22] C. A. Mead, Solid-State Electron. **9**, 1023 (1966).
[23] W. Mönch, J. Appl. Phys. **80**, 5076 (1996).
[24] W. Mönch, Appl. Surf. Sci. **92**, 367 (1996).
[25] J. Treusch, P. Eckerl, and O. Madelung, in Proc. Int. Conf. II–VI Semiconducting Compounds, edited by D. G. Thomas and W. A. Benjamin, New York, 1967.
[26] S. G. Louie, J. Chelikowsky, and M. L. Cohen, Phys. Rev. B **15**, 2154 (1977).